J Plant Growth Regul (2011) 30:467–479
DOI 10.1007/s00344-011-9209-9

CML24 is Involved in Root Mechanoresponses and Cortical Microtubule Orientation in *Arabidopsis*

Yichuan Wang · Bochu Wang · Simon Gilroy · E. Wassim Chehab · Janet Braam

Received: 26 December 2010 / Accepted: 5 April 2011 / Published online: 24 June 2011

Abstract Mechanostimuli can influence plant root system architecture by causing alterations in the root tip growth direction and triggering lateral root initiation. However, how a plant root senses and translates mechanostimulation into appropriate growth and/or developmental responses remains largely unclear. The fast expression induction and transcript turnover of the *Arabidopsis TCH* genes by touch stimulation suggest that the *TCH* genes may function in mechano-related events. However, the physiological functions of the *TCH* genes in *Arabidopsis* mechanoresponses remain undetermined. Here we screened a suite of *tch* mutants by characterizing their root growth behaviors on hard-agar surfaces. Two *calmodulin-like 24* (*CML24* or *TCH2*) mutants, *cml24-2* and *cml24-4*, exhibited reduced root length, biased skewing, and altered epidermal cell file rotation (CFR) phenotypes compared with wild type (Col-0). The mutant phenotypes were dependent on hard-agar surface contact and disappeared when seedlings were grown in liquid medium. Abnormal glass barrier responses of *cml24* mutants further indicate touch response defects. Pharmacological tests revealed differential sensitivity of *cml24* mutants to microtubule-targeted agents. Nonadditive effects of mutations in *CML24* and transgenic expression of a functional microtubule label, MBD-GFP, on root skewing and CFR phenotypes suggest a potential microtubule-related role of CML24. *In vivo* visualization of microtubule structures with the MBD-GFP reporter revealed altered cortical microtubule orientation in the epidermal cells in *cml24-4*. Our observations indicate that CML24 has a role in *Arabidopsis* root mechanoresponses, possibly through the regulation of cortical microtubule orientation.

Keywords Mechanoresponse · Root skewing · Barrier response · *TCH* genes · Microtubules · *Arabidopsis*

Electronic supplementary material The online version of this article (doi:10.1007/s00344-011-9209-9) contains supplementary material, which is available to authorized users.

Y. Wang · B. Wang (✉)
Key Laboratory of Biorheological Science and Technology (Chongqing University), Ministry of Education, Bioengineering College, Chongqing University, Chongqing 400030, China
e-mail: wangbc@cqu.edu.cn

Y. Wang
e-mail: mycqu@163.com

Y. Wang · E. Wassim Chehab · J. Braam (✉)
Department of Biochemistry and Cell Biology, Rice University, Houston, TX 77005, USA
e-mail: braam@rice.edu

E. Wassim Chehab
e-mail: ewchehab@rice.edu

S. Gilroy
Department of Botany, University of Wisconsin at Madison, Madison, WI 53706, USA
e-mail: sgilroy@wisc.edu

Introduction

As plant roots grow through the soil, they encounter a variety of mechanostimuli, including lateral pressure, friction by soil particles, and impedance by physical barriers, and gravity (Fasano and others 2002). Appropriate perception and response to these mechanostimuli substantially contribute to the adaption and survival of plant roots to local soil environment (Monshausen and Gilroy 2009a). Although positive gravitropism enables the root system to penetrate deeper into the soil, the perception and response to touch stimuli allow roots to avoid impenetrable soil

surfaces or objects and navigate around through more passable, less dense regions, which may also have greater permeability for air, water, and nutrient diffusion. Therefore, understanding the cellular and molecular bases of the regulation of plant root growth and development by mechanostimuli is of great importance not only to fundamental plant biology but also to agricultural practice.

Complex biotic and abiotic conditions and the opaque nature of soil present technical challenges in investigating the physiological impacts of mechanostimuli on plant roots (Dorlodot and others 2007). These problems can be circumvented by plant growth on homogeneous sterile growth medium solidified with macromolecular gelling agents. *Arabidopsis* seedlings grown on impenetrable agar surfaces produce two characteristic root growth patterns, waving and skewing (Okada and Shimura 1990; Rutherford and Masson 1996). Waving consists of repetitive sinusoidal undulations along the forward growth axis (Okada and Shimura 1990), and skewing is deviation of the net growth axis from the gravitational direction (Rutherford and Masson 1996). The major forces thought to contribute to these two growth patterns are gravity and the touch stimulation from the agar surfaces (Oliva and Dunand 2007), although convincing evidence suggests that other growth conditions can also affect aspects of root waving and skewing (Buer and others 2000, 2003). Embedding a horizontal impenetrable obstacle in front of *Arabidopsis* root tips penetrating Phytagel medium reveals another mechano-induced root growth behavior, the barrier response (Massa and Gilroy 2003). In the barrier response, *Arabidopsis* roots adopt a steplike growth pattern when they encounter the obstacle, with only the very tips remaining in contact with the barrier surface and the more proximal root segment positioned parallel to the barrier surface (Massa and Gilroy 2003). This altered growth behavior is proposed to be a touch-induced inhibition on gravity perception or response and may enable the fine navigation ability of plant roots during growth through soil-rock mixtures (Massa and Gilroy 2003). In addition to primary root directional growth, root branching can also be affected by mechanical forces. Lateral roots emerge from the convex side of a curved root, whether the curvature is formed by waving, gravitropism, or physical bending (Ditengou and others 2008; Richter and others 2009). Despite these well-recognized effects of mechanostimuli on plant root growth and development, the molecular mechanisms of mechanoperception and mechanoresponse remain largely unknown (Monshausen and Gilroy 2009a, b).

Transcriptional analyses of plant responses to mechanical stimuli have provided a vast collection of candidate genes that may function in different stages of plant mechanoresponses (Braam and Davis 1990; Braam 1992; Lee and others 2005). Among these genes are the four original *TCHs* (touch inducible genes). *TCH1-3* encode calmodulin (CaM) and calmodulin-like (CML) proteins, which suggests potential involvement of Ca^{2+} and potential Ca^{2+} receptors in *Arabidopsis* mechanoresponses. Although recent evidence implicates Ca^{2+} as an early trigger of the complex plant mechanotransduction pathways leading to appropriate mechanoresponses, such as lateral root initiation (Monshausen and others 2009; Richter and others 2009), the mechano-related functions of *TCHs* have not been elucidated.

In the present work we took advantage of root waving and skewing assays to explore the potential mechanoresponse functions of the CaM and CaM-related *TCH* genes (*CaM2* as *TCH1*, *CML12* as *TCH3*, and *CML24* as *TCH2*) in *Arabidopsis* root behaviors using a reverse genetic approach. We found that all the *tch* mutants tested showed normal root-waving ability and gravitropism. However, two *cml24* point mutants, shown previously to exhibit distinct phenotypic consequences (Tsai and others 2007), are shown here to demonstrate hard-agar surface-dependent root skewing and epidermal cell file rotation (CFR) alterations relative to wild type. In addition, the *cml24* mutants were not able to perform wild-type root responses to growth barriers. Pharmacological and genetic interaction analyses, as well as in vivo microtubule visualization, are consistent with the hypothesis that the *cml24* phenotypes may be due to disturbed regulation of cortical microtubule orientation.

Materials and Methods

Plant Material and Growth Conditions

cam2-1 (SALK-066990) and *cml12-2* (SALK-090554) are mutant lines for *TCH1* and *TCH3*, respectively. *cml24-2* and *cml24-4*, two functionally perturbed point mutants for *TCH2* (*CML24*), were described previously (Tsai and others 2007). *Arabidopsis thaliana* seeds were surface-sterilized with 70% ethanol for 1 min and half-strength bleach for 10 min. Sterilized seeds were cold-treated at 4°C for 2 days before being sown on growth medium containing half-strength Murashige and Skoog medium and 15 g/l sucrose and solidified with 12 g/l type E agar (Sigma, product No. A4675), pH 5.8. The plates were sealed with micropore tape and grown at 22°C with a 16 h light/8 h dark cycle for 7 days before imaging. In all skewing experiments, plates were tilted 15° back from the vertical.

For liquid-grown seedlings, seeds were germinated and grown in medium with the same nutrient composition as the plates except without agar, with each seedling in an independent 10-ml test tube with 5 ml medium. No shaking was applied during growth.

For microtubule agent treatments, seedlings were grown on medium supplemented with microtubule agents at indicated concentrations. Stock solutions of oryzalin (Ultra Scientific, product No. ULPST-1570) and taxol (MP Biomedicals, product No. IC19353205) were prepared in dimethylsulfoxide (DMSO). DMSO concentrations in all samples were adjusted to 0.03% (v/v); no differences were observed between this DMSO concentration and no-DMSO control.

Barrier response was performed as previously described (Massa and Gilroy 2003). Seedlings were grown in 0.5% (w/v) Phytagel (Sigma, product No. P8169) solidified medium in a near-vertical Petri dish. On days 5–7 post germination, sterile cover glass pieces were then inserted into the Phytagel, approximately 2 mm away from the root tip and perpendicular to both the growing root and the surface of the Petri dish. Two-minute-interval video frames were then recorded by Proscope HR (Bodelin Technologies, Lake Oswego, OR, USA) up to 10 h after the root tip began touching the barrier surface.

Root Skewing and Cell File Rotation (CFR) Quantification

For root-skewing angle measurements, photographic images were taken above each plate with an Olympus FE-320 digital camera. Skewing angle was defined as the angle between the gravitational vector and the growth vector starting from the shoot-root junction to the root tip. Leftward skewing to the gravitational vector was scored as negative and rightward skewing to the gravitational vector was scored as positive.

Close-up images for CFR measurement were also captured from above the plates with a Zeiss Axioskop microscope using a Zeiss AxioCam MRc5 digital camera and Zeiss AxioVision software (Carl Zeiss Inc., Germany). CFR was defined as the number of epidermal cell files that crossed a 1-mm-long line drawn down the longitudinal axis of the root, from 1.5 to 2.5 mm from the tip. Positive values represent right-handed CFR and negative values represent left-handed CFR.

In vivo Microtubule Observation

For *in vivo* microtubule visualization in epidermal root cells, wild-type (Col-0) seeds expressing *MBD-GFP* were kindly supplied by Elliot M. Meyerowitz, California Institute of Technology (Hamant and others 2008). Homozygous *MBD-GFP/cml24-2* and *MBD-GFP/cml24-4* plants were identified from progeny of genetic crosses of *MBD-GFP* with *cml24-2* and *cml24-4*, respectively. Five-day-old seedlings were used for microtubule observation. Fluorescent images were captured on a Leica TCS SP5 confocal microscope (Leica, Wetzlar, Germany) using the 488-nm line from an argon laser and a 515-nm-longpass emission filter. Serial confocal optical sections were taken at a 1-μm step size. For each seedling, imaging was finished within 15 min. Microtubule orientation was measured as the angle between a cortical microtubule and the transverse axis of an epidermal cell. Positive values represent right-handed orientation, whereas negative values represent left-handed orientation.

Projections of serial confocal sections and all digital measurements were performed with ImageJ software (NIH, USA), and all statistical analysis was performed by IBM® SPSS® Statistics software (IBM, Armonk, NY, USA).

Results

Characterization of *cml24* Mutant Root Phenotypes

When grown on the surface of hard-agar plates, *tch1* (*cam2-1*), *tch2* (*cml24-2*, *cml24-4*), and *tch3* (*cml12-2*) mutant roots displayed indistinguishable waving patterns from those of wild type (Fig. 1a–c, Supplementary Fig. 1a–c). *cam2-1* and *cml12-2* also showed similar root length and growth direction as wild type, with downward growth and only slight deviation to the left or the right (Supplementary Fig. 1a–c). In contrast, two functionally disrupted point mutant lines for *TCH2* (Tsai and others 2007), *cml24-2* and *cml24-4*, exhibited significantly altered root-skewing behavior relative to wild type; *cml24-2* roots skewed to the right (Fig. 1b) and *cml24-4* roots skewed to the left when viewed from above the plates (Fig. 1c). The opposite phenotypes of these two mutants are consistent with previous observations of distinct and opposing phenotypes of these two point mutants (Tsai and others 2007). Both *cml24* mutants also showed reduced root length compared with wild type (Fig. 1d). The root waving of wild type, *cml24-2*, and *cml24-4* and the skewing behaviors of *cml24-2* and *cml24-4* were no longer detectable if the roots penetrated into the agar medium (Fig. 1a–c). This recovery of straight vertical growth of the *cml24* mutant roots strongly suggests that their skewing behavior is surface contact-dependent rather than caused by defective gravitropism. On the other hand, *cml24* mutant roots maintained the shorter root phenotype relative to wild type when grown into the agar (Fig. 1b, c). The differential effect of surface versus in-agar growth on root length and skewing behaviors suggests that the mutant general growth defect can be uncoupled from the aberrant skewing behavior.

Previously reported *Arabidopsis* root skewing with fixed direction has been documented to be accompanied by epidermal cell file rotation (CFR) with preferential

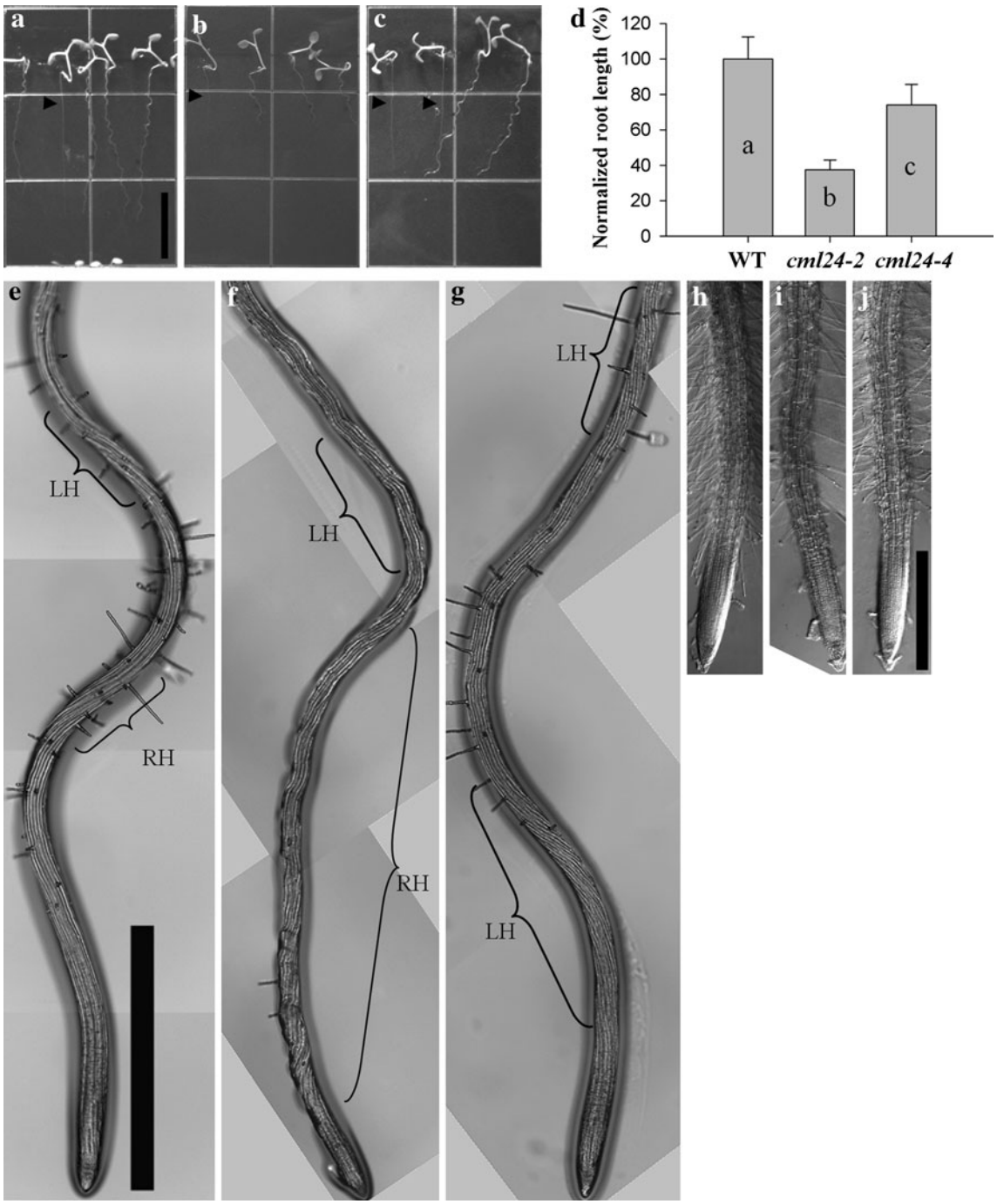

Fig. 1 Root phenotypes of wild type and *cml24* mutants. **a** Wild-type, **b** *cml24-2*, and **c** *cml24-4* seedlings grown on hard-agar surfaces. *Black arrowheads* indicate roots grown into the agar; note the absence of waving and skewing in agar-penetrated roots. **d** Normalized root length to average wild-type root length. Data are means ± SD ($n > 40$); letters in *bars* represent statistic differences ($P < 0.05$, LSD test). Close-up observation of CFR in **e** wild-type, **f** *cml24-2*, and **g** *cml24-4* roots grown on hard-agar surfaces; regions of CFR marked by braces. **e** Wild-type epidermal root cells undergo a left-handed (LH) cell file rotation (CFR) above a leftward root turn and a right-handed (RH) CFR above a rightward turn. **f**, **g** Examples of altered root CFR and direction of growth in *cml24-2* and *cml24-4*. **f** *cml24-2* root shows only mild left-handed (LH) CFR followed with a leftward turn, and then a prolonged right-handed (RH) CFR. **g** *cml24-4* root lacks a detectable right-handed CFR before the rightward turn. No detectable CFR was found in **h** wild-type, **i** *cml24-2*, and **j** *cml24-4* roots when seedlings are grown in shake-free liquid medium. *Scale bars* 10 mm (*a–c*), 1 mm (*e–g*), 0.5 mm (*h–j*)

handedness (Oliva and Dunand 2007), although exceptions have also been described (Buer and others 2003). Under our growth conditions, our observations were consistent with the typical correlations described by Oliva and Dunand (2007). Thus, in a wavy wild-type root, a leftward turn was usually preceded by a region of left-handed CFR, and a rightward turn was usually preceded by a region of right-handed CRF (Fig. 1e). However, the left-handed CFR in *cml24-2* roots (Fig. 1f) and the right-handed CFR in *cml24-4* roots (Fig. 1g) were much milder than those of the opposite handedness, resulting in net CFR with biased handedness (Table 1). Due to technical limitations, we were not able to clearly document the cell file features of those roots that had grown into the agar. However, when grown in liquid medium, the biased root CFR handedness disappeared in the *cml24* mutants (Fig. 1i, j). Instead, they showed relatively straight cell files parallel to the longitudinal root axis, as seen in wild type (Fig. 1h). The differential behaviors of the *cml24* mutant roots on agar surfaces versus in liquid media strongly suggest that their biased CFR may be dependent on physical contact between the root and agar surface.

Glass Barrier Responses of *cml24* Mutant Roots

The hard-agar surface-dependent root skewing and CFR features of *cml24* mutants suggest that CML24 function may be necessary for root tip touch responses in *Arabidopsis*. To test this hypothesis, we compared the glass barrier responses (Massa and Gilroy 2003) between wild-type Col-0 and the two *cml24* mutants. When wild-type roots encounter a glass barrier that is set perpendicular to the root growth direction, the roots reproducibly form a step-like growth pattern, consisting of two bends separated by a root segment nearly parallel to the glass barrier surface (Fig. 2a). In contrast, the barrier responses of the *cml24* mutant roots were aberrant (Fig. 2b–g). The second bends in the *cml24* mutant roots were typically flatter than those of wild type; some *cml24* mutant roots nearly failed to form the second bend (Fig. 2b-g). As a consequence, whereas wild-type roots keep only one point (the root tip) in contact with the barrier surface (Fig. 2a, Supplementary movie 1), many *cml24* mutant roots bent beyond parallel to the barrier (Fig. 2b, c) or directly contacted the barrier with root regions between the typical two bends (Fig. 2d, e) or directly contacted the barrier along the root after the first bend (Fig. 2f, g, Supplementary movies 2, 3). All these abnormal root behavior patterns were observed in both *cml24* mutants, although quantitative analysis reveals that the second bends in *cml24-2* were generally flatter than those of *cml24-4* (Fig. 2h). These results confirm that both *cml24-2* and *cml24-4* display hard-surface touch defects.

Altered Sensitivity of Root Skewing of *cml24* Mutants to Microtubule-targeted Agents

Most, if not all, of the previously reported *Arabidopsis* mutants with biased root skewing and altered CFR have defects in microtubule organization or turnover dynamics (Ishida and others 2007b; Sedbrook and Kaloriti 2008). To test whether the above-described phenotypes of the *cml24* mutants are also related to microtubule functions, we examined the effects of the microtubule-destabilizing agent oryzalin and microtubule-stabilizing agent taxol on root-skewing behavior. Oryzalin supplementation of growth medium did not significantly change the growth direction

Table 1 Quantitative characterization of wild-type and *cml24* mutant root phenotypes under various conditions

	Control	0.1 μM oryzalin	1 μM taxol
Wild-type angle	−2.8 ± 2.8	−5.5 ± 8.9	−13.6 ± 4.6 b
cml24-2 angle	16.0 ± 5.8 a	17.5 ± 9.3	−6.4 ± 7.4 b
cml24-4 angle	−20.7 ± 6.2 a	4.5 ± 4.3 b	−26.0 ± 5.2
wild-type CFR	−3.3 ± 2.9	−4.7 ± 1.1	−9.7 ± 6.5 b
cml24-2 CFR	5.8 ± 4.0 a	6.0 ± 3.9	ND
cml24-4 CFR	−8.0 ± 5.9 a	−2.9 ± 4.7 b	−14.2 ± 5.8 b
MBD-GFP angle	43.3 ± 6.0	ND	ND
*MBD-GFP/cml24-2*angle	41.5 ± 4.6	ND	ND
MBD-GFP/cml24-4 angle	50.9 ± 4.8 a	ND	ND
MBD-GFP CFR	4.1 ± 3.6	ND	ND
MBD-GFP/cml24-2 CFR	2.9 ± 2.4	ND	ND
MBD-GFP/cml24-4 CFR	7.8 ± 1.8 a	ND	ND

Data are means ± SD, $n \geq 15$ for each. Similar results were obtained in at least 2 independent experiments. Letters after numbers present statistic difference ($P < 0.05$, LSD-test), 'a' indicates difference from wild type under control conditions, and 'b' indicates difference between experimental treatments of the same genotype. *ND* indicates that experiment was not conducted

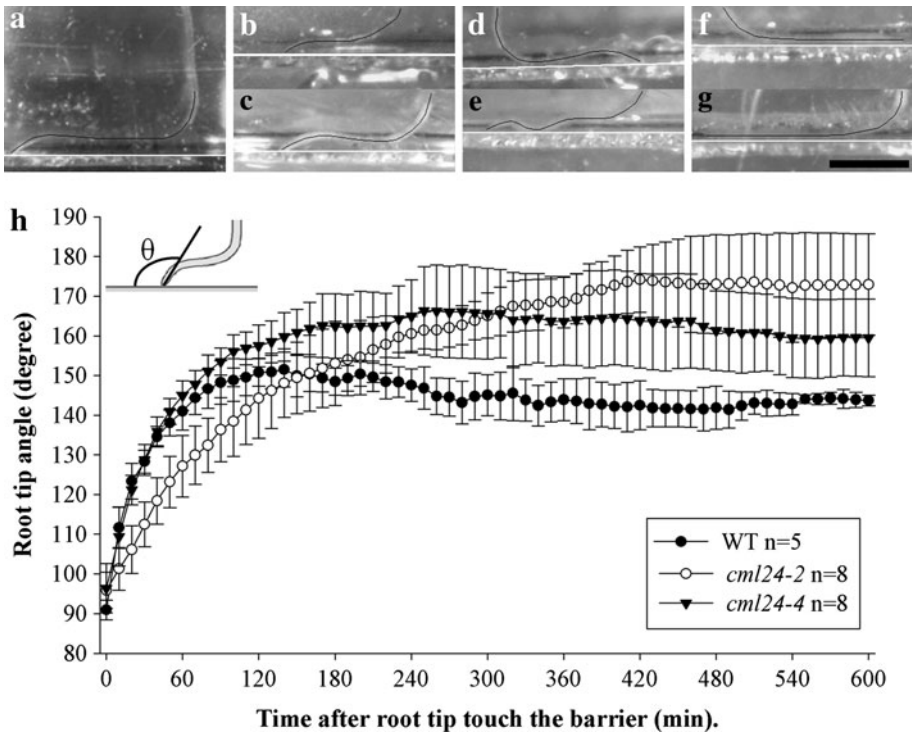

Fig. 2 Barrier responses of wild type and *cml24* mutants. Final frames of 10-h time-lapse movies made of **a** wild-type, **b**, **d**, **f** *cml24-2*, and **c**, **e**, **g** *cml24-4* roots after the root tips touch the grass barrier. *Black lines* indicate the middle axis of each root and *white lines* indicate the upper surface of glass barriers. **a** Wild-type roots performed the typical steplike barrier response. **b** Some *cml24-2* and **c** *cml24-4* roots perform a similar steplike barrier response but the root segments between the two bends come closer to the glass barrier than in the wild type. **d**, **e** Examples of *cml24-2* and *cml24-4* roots, respectively, with root segments between two bends contacting the glass barrier. **f**, **g** Examples of *cml24-2* and *cml24-4* roots, respectively, that fail to form a second bend; instead the length of root region after the first bend is in direct contact with the barrier. **h** Root tip angles of wild type, *cml24-2*, and *cml24-4* relative to horizontal barriers were measured over time. Data are means ± SD. Inset diagram indicates the root tip angle *h* measured. *Scale bars* 1 mm

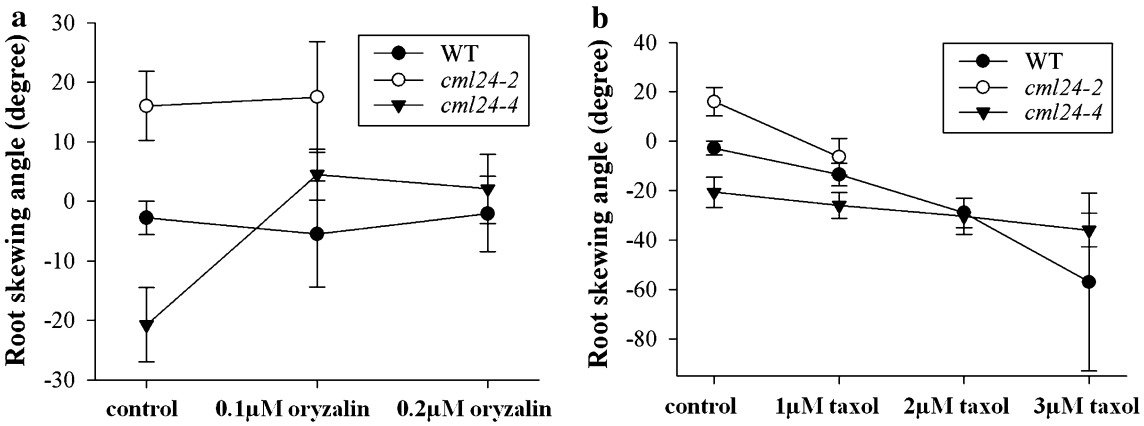

Fig. 3 Effects of microtubule-targeted agents **a** oryzalin and **b** taxol on skewing angle of wild type and *cml24* mutants. Leftward skewing from the vertical was scored negative and rightward skewing from the vertical was scored positive. Data are means ± SD ($n > 40$)

or CFR of wild-type or *cml24-2* roots (Fig. 3a, Table 1). On the other hand, the leftward skewing and left-handed CFR of *cml24-4* roots were suppressed on 0.1 μM oryzalin-supplemented agar surface (Fig. 3a, Table 1), indicating that *cml24-4* is more sensitive to oryzalin relative to wild type and *cml24-2*.

Taxol supplementation of growth medium induced leftward root skewing of both wild type and the two *cml24* mutants (Fig. 3b). Although *cml24-4* roots skewed significantly more leftward ($P < 0.05$, *t*-test) relative to wild-type roots in control conditions, they showed similar intensity ($P = 0.884$, *t*-test) of leftward skewing in 2 μM taxol, and

cml24-4 roots were significantly less ($P < 0.05$, *t*-test) leftward relative to wild-type roots in 3 μM taxol (Fig. 3b), indicating that *cml24-4* is less sensitive to taxol than wild type. In addition, 1 μM taxol induced a significant left-handed CFR in wild type, enhanced the preexisting left-handed CFR in *cml24-4*, and shifted the right-handed CFR in *cml24-2* to left-handed (Table 1). The same concentration of taxol also induced a substantial number of swollen root epidermal cells in *cml24-2* (Supplementary Fig. 2b), which made the quantification of CFR of *cml24-2* in this treatment difficult. These swollen root cells were not seen in wild type or *cml24-4* at 1 μM taxol supplementation (Supplementary Fig. 2a, c); these results suggest that *cml24-2* is more sensitive to taxol relative to wild-type and *cml24-4*. Due to the relative severe growth defect of *cml24-2* (Fig. 1b, d), together with the inhibitory effects of microtubule drugs, we were not able to accurately evaluate the skewing intensity of *cml24-2* on the higher concentrations of oryzalin and taxol. For the same reason, we quantified the CFR of only seedlings grown under control or low-level drug treatment conditions (Table 1).

In vivo Visualization of Microtubule Structures by MBD-GFP

The similarity of the skewing and CFR phenotypes of *cml24* mutants to previously reported microtubule-associated mutants (Ishida and others 2007b; Sedbrook and Kaloriti 2008), together with their differential sensitivity to microtubule-targeted agents, prompted us to look for more direct evidence that CML24 may affect microtubule organization. We employed a commonly used microtubule-labeled transgenic line in the wild-type Col-0 background, *MBD-GFP* (GFP fusion with Microtubule-Binding Domain of mammalian Microtubule-Associated Protein 4) (Marc and others 1998), to image and compare in vivo microtubule organization among roots of wild type and *cml24* mutants.

The *MBD-GFP* transgenic plants had good labeling of the cortical microtubule structure of the root epidermal cells (Figs. 4, 5), as previously reported (Bruaene and others 2004). We observed, however, that the *MBD-GFP* transgenic roots revealed strong rightward skewing accompanied by a preferential right-handed CFR (Fig. 6a, e, Table 1). These phenotypes were proposed to be caused by the microtubule polymerization and stabilization functions of MAP4 (Olson and others 1995; Hashimoto 2002). We reasoned that if CML24 has a function in root growth behavior unrelated to microtubule functions, then combining the *cml24* mutants with the *MBD-GFP* transgene would result in an additive effect on root-skewing behavior, yielding a stronger rightward skewing phenotype of the *MBD-GFP/cml24-2* homozygous seedlings and an intermediate skewing phenotype of *MBD-GFP/cml24-4* homozygous seedlings relative to the respective parent lines. Surprisingly, all of the homozygous F3 plants of *MBD-GFP/cml24-4* (Fig. 6c, g, Table 1), but not of *MBD-GFP/cml24-2* (Fig. 6b, f, Table 1), showed exaggerated rightward root skewing and enhanced right-handed CFR phenotypes relative to the *MBD-GFP*. That is, although the *cml24-4* mutation on its own causes leftward root skewing (Fig. 1c), the *cml24-4* mutation in the presence of the *MBD-GFP* transgene enhances the MBD-GFP-induced rightward root skewing (Fig. 6a, c). Root phenotypes of *MBD-GFP/cml24-2* were largely indistinguishable from those of *MBD-GFP* (Fig. 6b, f, Table 1). However, the severe root growth defect of *cml24-2* was substantially rescued by the presence of *MBD-GFP* (compare Figs. 1d, 6d). This rescuing effect is not seen when other non-microtubule-related GFP-fusion proteins are produced in *cml24-2* (Supplementary Fig. 3). These results provide genetic evidence that CML24 may have a microtubule-related function.

Despite the strong rightward *MBD-GFP* root-skewing phenotype when grown on agar surfaces, the cortical microtubules in the *MBD-GFP* elongation zone epidermal cells are predominantly transverse in orientation, with slight deviations of individual bundles (Fig. 4a, d, g), similar to that described for nontransgenic wild type using immunofluorescence (Sugimoto and others 2000). Cells with slight oblique cortical microtubule orientation, either left-handed or right-handed, were detected in the middle elongation zone (Fig. 4d) and more frequently in the basal elongation zone (Fig. 4a). Quantitative analysis of cortical microtubule orientation in epidermal cells of the elongation zone (from distal elongation zone to basal elongation zone) revealed that *MBD-GFP* harbored slightly more microtubules with right-handed orientation than with left-handed orientation (Fig. 7a). Similar cortical microtubule configurations were seen in *MBD-GFP/cml24-2* roots (Figs. 4b, e, h, 7a). In *MBD-GFP/cml24-4*, however, there were more microtubules with left-handed orientation than with right-handed orientation (Fig. 7a). In addition, *MBD-GFP/cml24-4* cells with left-handed microtubule orientation were seen in the distal elongation zone (Fig. 4i) and extended through the entire elongation zone (Fig. 4f, c). Statistical analysis also revealed that the average cortical microtubule orientation angle of *MBD-GFP/cml24-4* cells is significantly more left-handed relative to that of *MBD-GFP* and *MBD-GFP/cml24-2* cells (Fig. 7b). These results suggest that CML24 may have a role in the regulation of cortical microtubule orientation in the root elongation zone.

To investigate the potential correlation between altered microtubule orientation and abnormal root mechanoresponsiveness of the *cml24* mutants, we also compared the

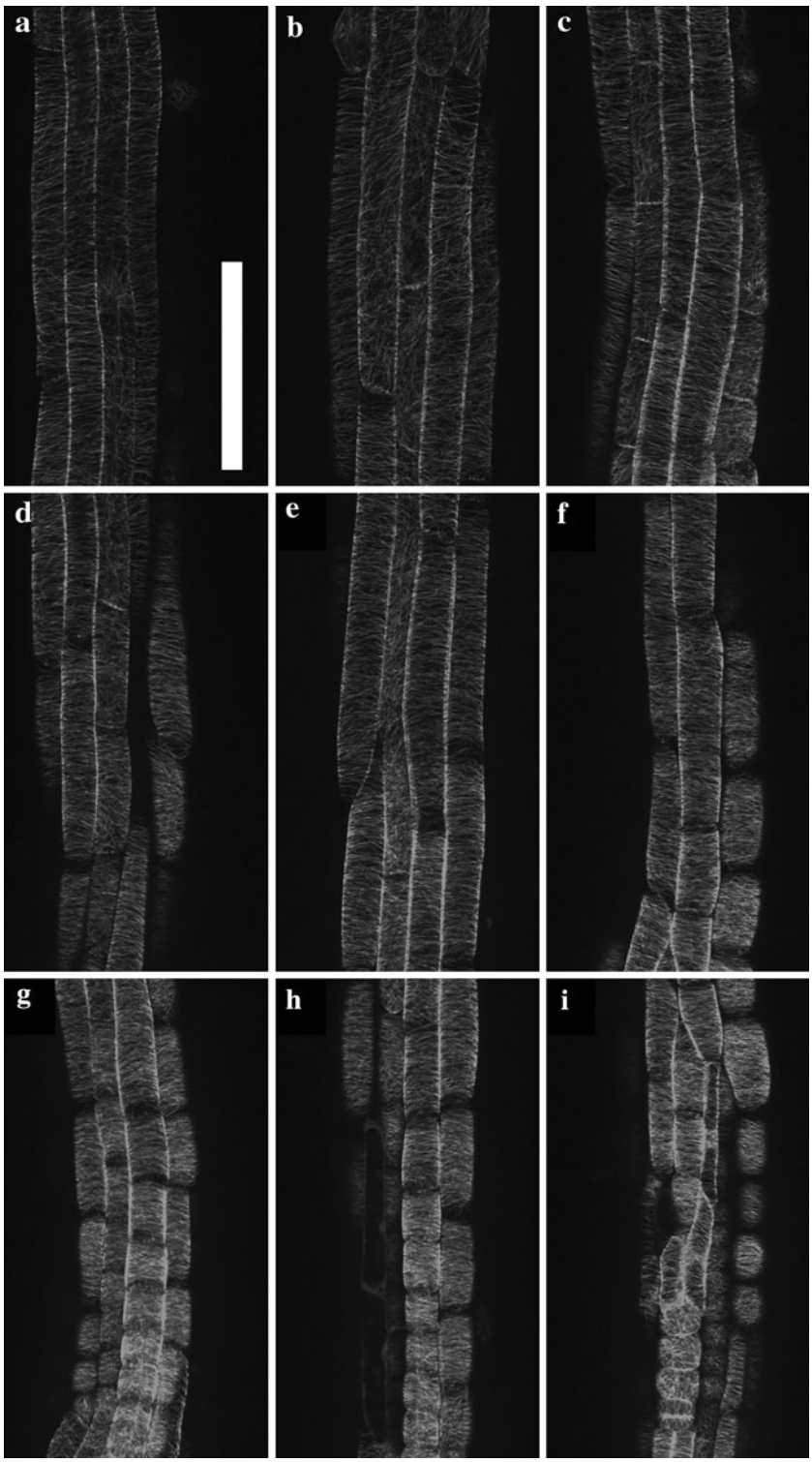

Fig. 4 Cortical microtubule orientation of *MBD-GFP*, *MBD-GFP/cml24-2*, and *MBD-GFP/cml24-4* seedlings grown on hard-agar surfaces. Cortical microtubule arrays in **a–c** are from the basal elongation zone, in **d–f** from the central elongation zone, and in **g–i** from the distal elongation zone. **a, d, g** Images from a representative *MBD-GFP* root. **b, e, h** Images from a representative *MBD-GFP/cml24-2* root. **c, f, i** Images from a representative *MBD-GFP/cml24-4* root. *Scale bars* 100 μm

microtubule orientation of *MBD-GFP*, *MBD-GFP/cml24-2*, and *MBD-GFP/cml24-4* seedlings grown in liquid medium. Consistent with the reduced net CFR in nontransgenic wild type and *cml24* mutants when grown in liquid medium (Fig. 1h–j), no detectable CFR was observed in *MBD-GFP* (Fig. 6h), *MBD-GFP/cml24-2* (Fig. 6i), or *MBD-GFP/cml24-4* (Fig. 6j) under similar conditions. Overall, similar microtubule orientation patterns were observed in *MBD-GFP* (Fig. 5a, d, g), *MBD-GFP/cml24-2* (Fig. 5b, e, h), and *MBD-GFP/cml24-4* (Fig. 5c, f, i), although the average

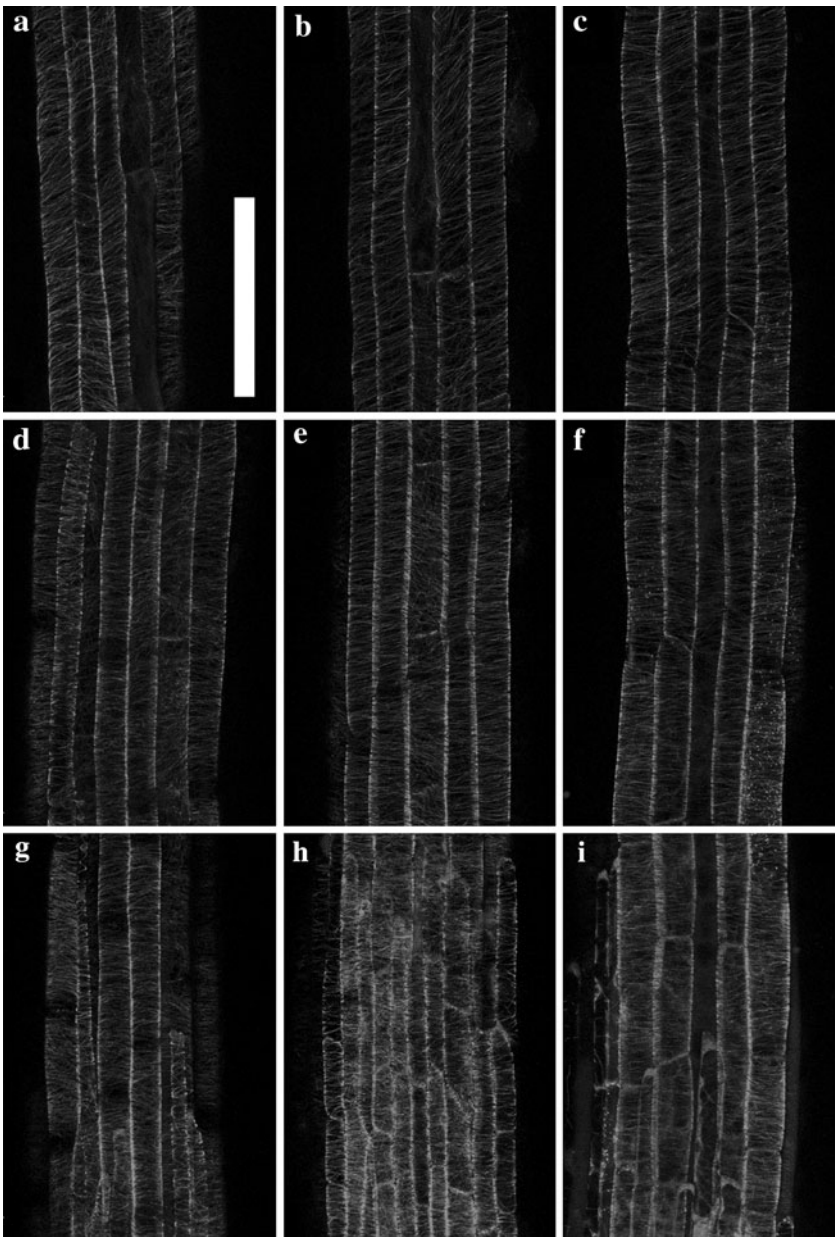

Fig. 5 Cortical microtubule orientation of *MBD-GFP*, *MBD-GFP/cml24-2*, and *MBD-GFP/cml24-4* seedlings grown in liquid medium. Cortical microtubule arrays in **a–c** are from the basal elongation zone, in **d–f** from the central elongation zone, and in **g–i** from the distal elongation zone. **a, d, g** Images from a representative *MBD-GFP* root. **b, e, h** Images from a representative *MBD-GFP/cml24-2* root. **c, f, i** Images from a representative *MBD-GFP/cml24-4* root. *Scale bars* 100 μm

microtubule orientation of liquid-grown *MBD-GFP/cml24-4* was slightly less right-handed than those of *MBD-GFP* and *MBD-GFP/cml24-2* (Fig. 7b). Quantitative analysis revealed net right-handed microtubule orientation in all three genotypes and there were no significant differences between the agar-grown and liquid-grown *MBD-GFP* and *MBD-GFP/cml24-2* roots (Fig. 7b). In contrast, microtubule orientation in *MBD-GFP/cml24-4* was significantly different between roots grown on hard-agar surfaces versus in liquid medium (Fig. 7). Taken together, these results indicate that the hard-agar surface-dependent altered skewing and CFR phenotype of *cml24* mutants may be attributed to the function of CML24 in mediating the regulation of cortical microtubule orientation in the root elongation zone.

Discussion

Although increasing evidence demonstrates a fundamental function of mechanostimuli in the regulation of plant growth and development, the molecular basis for the plant mechanoresponse is still largely unknown (Telewski 2006; Chehab and others 2009; Monshausen and Gilroy 2009a, b; Coutand 2010). To explore the potential function of the *TCH* genes in

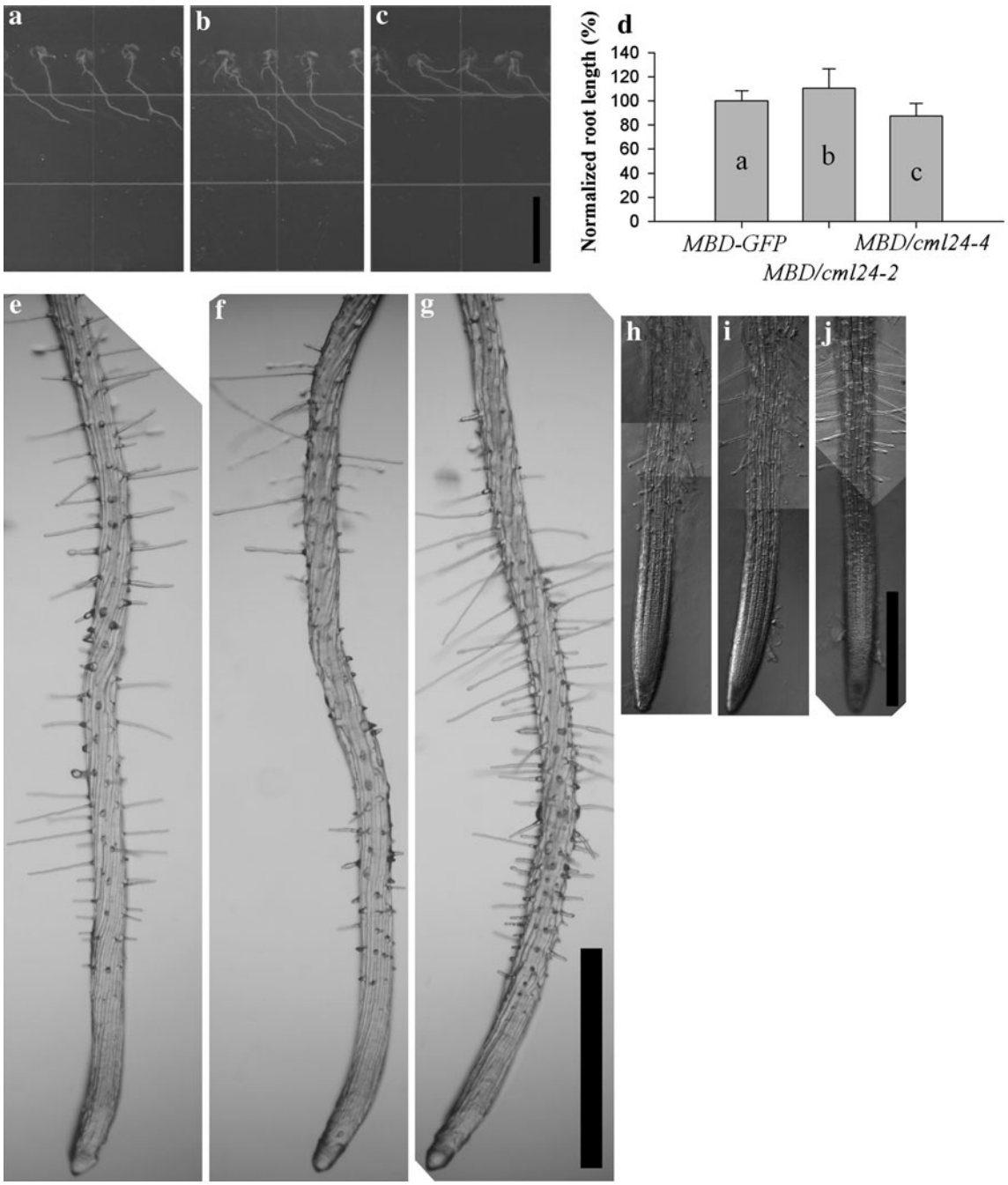

Fig. 6 Root phenotypes of *MBD-GFP*, *MBD-GFP/cml24-2*, and *MBD-GFP/cml24-4*. **a** *MBD-GFP*, **b** *MBD-GFP/cml24-2*, and **c** *MBD-GFP/cml24-4* seedlings grown on hard-agar surfaces. **d** Normalized root length to average *MBD-GFP* root length. Data are means ± SD ($n > 40$); letters in bars represent statistical differences ($P < 0.05$, LSD test). Close-up observation of CFR in **e** *MBD-GFP*, **f** *MBD-GFP/cml24-2*, and **g** *MBD-GFP/cml24-4* roots grown on hard-agar surfaces; note the constant right-handed CFR in all three *MBD-GFP* transgenic lines. **e** *MBD-GFP* and **f** *MBD-GFP/cml24-2* show similar intensity of right-handed CFR, while **g** *MBD-GFP/cml24-4* shows enhanced right-handed CFR relative to **e** *MBD-GFP* and **f** *MBD-GFP/cml24-2*. No detectable CFR was found in **h** *MBD-GFP*, **i** *MBD-GFP/cml24-2*, and **j** *MBD-GFP/cml24-4* roots when seedlings are grown in shake-free liquid medium. *Scale bars* 10 mm (*a–c*), 1 mm (*e–g*), 0.5 mm (*h–j*)

Arabidopsis root mechanoresponses, we conducted root-waving and root-skewing assays on a collection of *tch* mutants and further confirmed the defective touch responses of two *cml24* mutants with the barrier-response assay.

Root waving and skewing on hard-agar surfaces are commonly considered two growth responses to the integrated stimuli of gravity and touch between root tip and agar surface (Oliva and Dunand 2007). Although waving

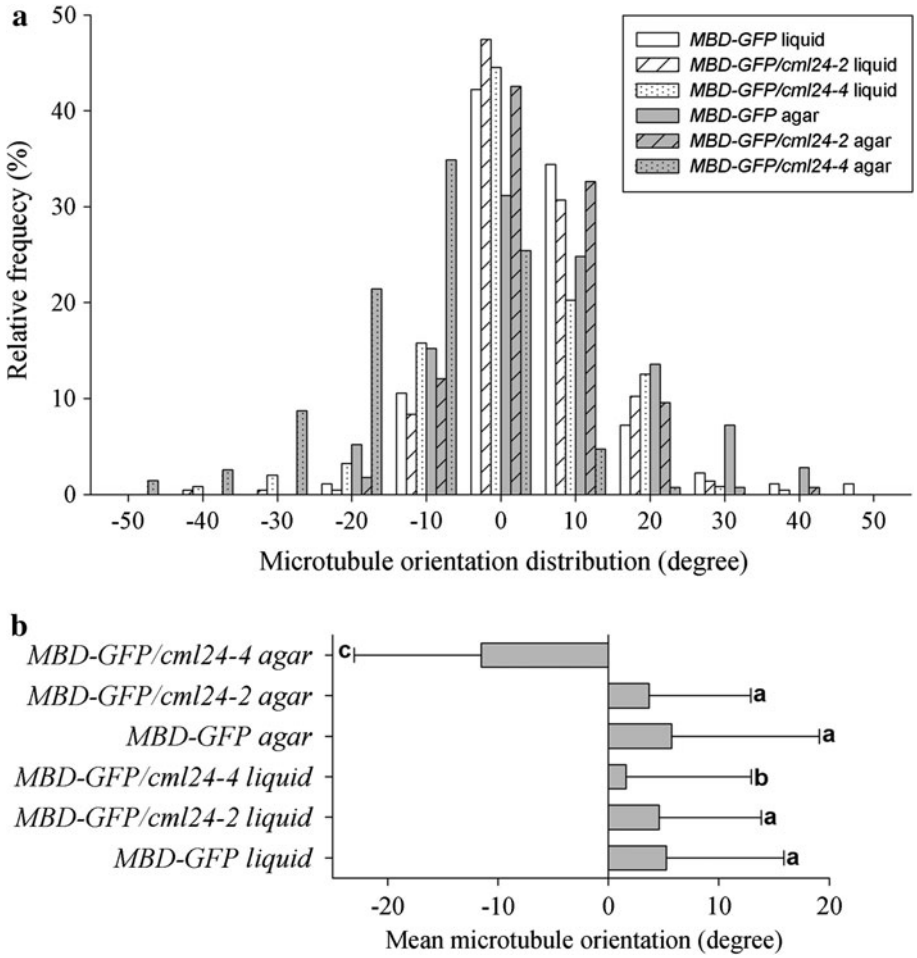

Fig. 7 Quantification of cortical microtubule orientation of *MBD-GFP*, *MBD-GFP/cml24-2*, and *MBD-GFP/cml24-4* seedlings grown on hard-agar surfaces and in liquid medium. **a** Relative frequency of cortical microtubule orientation in epidermal cells of root elongation zone ($n \geq 250$). **b** Average cortical microtubule orientation in epidermal cells of root elongation zone. Data are means ± SD ($n \geq 250$). 0 indicates transverse orientation, negative values indicate leftward orientation, and positive values indicate rightward orientation

and skewing are two growth behaviors usually occurring at the same time, skewing can also be found without obvious waving (Yuen and others 2005). Our observation also supports uncoupling of these two behaviors. All the mutants tested in this work have similar waving behaviors as the wild type. However, two *cml24* mutants showed significant skewing with fixed directions (Fig. 1b, c). Most previously characterized skewing mutants also show preferential epidermal CFR (Ishida and others 2007b; Oliva and Dunand 2007). We also observed net right-handed CFR with right skewing in *cml24-2* and net left-handed CFR with left skewing in *cml24-4* (Table 1). Although we did not detect abnormal waving or significant skewing in *cam2* and *cml12* mutants, the potential functional overlap of the *Arabidopsis CAMs* and *CMLs* may mask phenotypic consequences of these mutations (McCormack and Braam 2003; Delk and others 2005; McCormack and others 2005). Future examination of plants with combined mutations in *CAMs* and *CMLs* may help test this hypothesis.

According to the Oliva and Dunand model, a defective response in either touch or gravity can lead to altered growth behavior of *Arabidopsis* roots when grown on agar surfaces (Oliva and Dunand 2007). The normal downward growth patterns of the *cml24* mutants after penetrating the agar rule out a significant defect in gravitropism (Fig. 1b, c). In contrast, the lack of CFR detection in the relatively touch-free condition of liquid medium suggests that the skewing and CFR phenotypes of these mutants may be attributed to an impaired response to touch (Fig. 1i, j). This hypothesis is supported by our observation that both of the *cml24* mutants were not able to form a normal steplike barrier response as was seen in the wild type (Fig. 2).

The interphase array of cortical microtubules of higher plant cells is believed to guide the deposition of cellulose microfibrils and thus control mechanical properties of the plant cell wall and direct the orientation of cell expansion (Lloyd and Chan 2002, 2008; Paredez and others 2006). More recent studies also demonstrated an important role of mechanical stress-reoriented cortical microtubules in shoot organ pattern formation (Hamant and others 2008; Heisler and others 2010). Although it is not clear whether mechanical stress also takes part in the skewing behavior of most microtubule-related mutants, similar correlation of

root-skewing direction and CFR handedness in the two *cml24* mutants with those of previously reported microtubule-related mutants (Furutani and others 2000; Thitamadee and others 2002; Yuen and others 2003; Abe and Hashimoto 2005; Ishida and others 2007a) suggests that microtubule-related defects arise when the normal function of CML24 is disturbed. This possibility is supported by the demonstrated differential sensitivity of the two *cml24* mutants, relative to wild type, to two commonly used microtubule-targeted agents, oryzalin and taxol. The differential response to these two agents suggests that the microtubule structure in *cml24-2* may be less stable compared with the wild type, whereas the microtubule structure in *cml24-4* may be more stable compared with the wild type. Secondly, combining the *cml24* mutations with a microtubule-stabilizing protein-encoding transgene, *MBD-GFP*, generated nonadditive effects on both skewing and CFR phenotypes.

Disruption of cortical microtubule-related function usually results in altered microtubule orientation (Sedbrook and Kaloriti 2008). Consistent with the lack of morphological differences between *MBD-GFP*/*cml24-2* and *MBD-GFP*, we also did not detect distinguishable microtubule features between them, when the seedlings were grown on agar surface or in liquid medium (Fig. 7a, b). However, *MBD-GFP*/*cml24-4* roots harbored more left-handed-oriented cortical microtubules and a net left-handed average orientation than *MBD-GFP* and *MBD-GFP*/*cml24-2* when seedlings were grown on a hard-agar surface, but not in liquid medium (Fig. 7a, b). This hard-agar surface-dependent change in cortical microtubule orientation supports the hypothesis that CML24 may have a role in root mechanoresponse via regulation of cortical microtubule orientation.

Early in vitro reports have provided evidence for opposing roles of CaM in plant microtubule organization (Cyr 1991; Fisher and Cyr 1993; Fisher and others 1996). The effect of CaM on microtubule organization was reported to be Ca^{2+} concentration-dependent, and the interaction between Ca^{2+}/CaM and microtubules was proposed to be indirect and mediated by other undefined proteins (Cyr 1991; Fisher and Cyr 1993; Fisher and others 1996). Similarly, CML24 may have a complex role in microtubule organization, reflected by the distinct effects of the two different *cml24* mutant isoforms. CML24, like CaM, may have multiple-target proteins that may be differentially affected by mutant protein isoforms. Elucidating the mechanism by which the two *cml24* mutant isoforms may differentially affect microtubule orientation during *Arabidopsis* root mechanoresponses will be a challenging aspect of our future work. Previous evidence supporting a potential role for CML24 in plant cytoskeleton regulation came from an in vitro screen using mammalian fibroblast actin stress fiber analysis (Abu-Abied and others 2006). Yet, the authors were unable to detect a direct binding of CML24-YFP with actin filaments in vitro. Instead, they found CML24-YFP, but not CAM2-YFP, bound to the IQ domain of *Arabidopsis* myosin VIII in a Ca^{2+}-dependent manner (Abu-Abied and others 2006). With increasing evidence of interaction between plant actin microfilaments and microtubules (Schwab and others 2003; Gossot and Geitmann 2007; Collings 2008), the potential role of CML24 in mechano-related physiological events involving cytoskeleton elements will also be an important future research direction.

Acknowledgments This material is based upon work supported by the National Science Foundation under grant Nos. MCB 0817976 (JB) and MCB-0641288, by the National Aeronautics and Space Administration under grant No. NNX09AK80G (SG), and the National Natural Science of China under grant No. 10872223 (BW). We thank Elliot M. Meyerowitz for kindly providing the *MBD-GFP* seeds, and Sarah Swanson and William Deery for technical support in imaging. We are grateful to Yu-Chang Tsai and Won-Gyu Choi for helpful discussions and to Liz Eich for isolation and characterization of the *cml12-2* mutant.

References

Abe T, Hashimoto T (2005) Altered microtubule dynamics by expression of modified alpha-tubulin protein causes right-handed helical growth in transgenic *Arabidopsis* plants. Plant J 43: 191–204

Abu-Abied M, Golomb L, Belausov E, Huang SJ, Geiger B, Kam Z, Staiger CJ, Sadot E (2006) Identification of plant cytoskeleton-interacting proteins by screening for actin stress fiber association in mammalian fibroblasts. Plant J 48:367–379

Braam J (1992) Regulation of expression of calmodulin and calmodulin-related genes by environmental stimuli in plants. Cell Calcium 13:457–463

Braam J, Davis RW (1990) Rain-, wind-, and touch-induced expression of calmodulin and calmodulin-related genes in *Arabidopsis*. Cell 60:357–364

Bruaene NV, Joss G, Oostveldt PV (2004) Reorganization and in vivo dynamics of microtubules during *Arabidopsis* root hair development. Plant Physiol 136:3905–3919

Buer CS, Masle J, Wasteneys GO (2000) Growth conditions modulate root-wave phenotypes in *Arabidopsis*. Plant Cell Physiol 41: 1164–1170

Buer CS, Wasteneys GO, Masle J (2003) Ethylene modulates root-wave responses in *Arabidopsis*. Plant Physiol 132:1085–1096

Chehab EW, Eich E, Braam J (2009) Thigmomorphogenesis: a complex plant response to mechano-stimulation. J Exp Bot 60: 43–56

Collings DA (2008) Crossed-wires: interactions and cross-talk between the microtubule and microfilament networks in plants. In: Nick P (ed) Plant microtubules 2008. Springer-Verlag, Berlin, pp 47–79

Coutand C (2010) Mechanosensing and thigmomorphogenesis, a physiological and biomechanical point of view. Plant Sci 179: 168–182

Cyr RJ (1991) Calcium calmodulin affects microtubule stability in lysed protoplasts. J Cell Sci 100:311–317

Delk NA, Johnson KA, Chowdhury NI, Braam J (2005) CML24, regulated in expression by diverse stimuli, encodes a potential Ca^{2+} sensor that functions in response to abscisic acid, daylength, and ion stress. Plant Physiol 139:240–253

Ditengou FA, Teale WD, Kochersperger P, Flittner KA, Kneuper I, van der Graaff E, Nziengui H, Pinosa F, Li X, Nitschke R, Laux T, Palme K (2008) Mechanical induction of lateral root initiation in *Arabidopsis thaliana*. Proc Natl Acad Sci USA 105:18818–18823

Dorlodot S, Forster B, Pages L, Price A, Tuberosa R, Draye X (2007) Root system architecture: opportunities and constraints for genetic improvement of crops. Trends Plant Sci 12:474–481

Fasano JM, Massa GD, Gilroy S (2002) Ionic signaling in plant responses to gravity and touch. J Plant Growth Regul 21:71–88

Fisher DD, Cyr RJ (1993) Calcium levels affect the ability to immunolocalize calmodulin to cortical microtubules. Plant Physiol 103:543–551

Fisher DD, Gilroy S, Cyr RJ (1996) Evidence for opposing effects of calmodulin on cortical microtubules. Plant Physiol 112: 1079–1087

Furutani I, Watanabe Y, Prieto R, Masukawa M, Suzuki K, Naoi K, Thitamadee S, Shikanai T, Hashimoto T (2000) The SPIRAL genes are required for directional control of cell elongation in *Arabidopsis thaliana*. Development 127:4443–4445

Gossot O, Geitmann A (2007) Pollen tube growth: coping with mechanical obstacles involves the cytoskeleton. Planta 226: 405–416

Hamant O, Heisler MG, Jonsson H, Krupinski P, Uyttewaal M, Bokov P, Corson F, Sahlin P, Boudaoud A, Meyerowitz EM, Couder Y, Traas J (2008) Developmental patterning by mechanical signals in *Arabidopsis*. Science 322:1650–1655

Hashimoto T (2002) Molecular genetic analysis of left-right handedness in plants. Philos Trans R Soc B 357:799–808

Heisler MG, Hamant O, Krupinski P, Uyttewaal M, Ohno C, Jonsson H, Traas J, Meyerowitz EM (2010) Alignment between PIN1 polarity and microtubule orientation in the shoot apical meristem reveals a tight coupling between morphogenesis and auxin transport. Plos Biol 8:e1000516

Ishida T, Kaneko Y, Iwano M, Hashimoto T (2007a) Helical microtubule arrays in a collection of twisting tubulin mutants of *Arabidopsis thaliana*. Proc Natl Acad Sci USA 104:8544–8549

Ishida T, Thitamadee S, Hashimoto T (2007b) Twisted growth and organization of cortical microtubules. J Plant Res 120:61–70

Lee D, Polisensky DH, Braam J (2005) Genome-wide identification of touch- and darkness-regulated Arabidopsis genes: a focus on calmodulin-like and *XTH* genes. New Phytol 165:429–444

Lloyd C, Chan J (2002) Helical microtubule arrays and spiral growth. Plant Cell 14:2319–2324

Lloyd C, Chan J (2008) The parallel lives of microtubules and cellulose microfibrils. Curr Opin Plant Biol 11:641–646

Marc J, Granger CL, Brincat J, Fisher DD, Kao TH, McCubbin AG, Cyr RJ (1998) A *GFP-MAP4* reporter gene for visualizing cortical microtubule rearrangements in living epidermal cells. Plant Cell 10:1927–1939

Massa GD, Gilroy S (2003) Touch modulates gravity sensing to regulate the growth of primary roots of *Arabidopsis thaliana*. Plant J 33:435–445

McCormack E, Braam J (2003) Calmodulins and related potential calcium sensors of *Arabidopsis*. New Phytol 159:585–598

McCormack E, Tsai YC, Braam J (2005) Handling calcium signaling: *Arabidopsis* CaMs and CMLs. Trends Plant Sci 10:383–389

Monshausen GB, Gilroy S (2009a) The exploring root—root growth responses to local environmental conditions. Curr Opin Plant Biol 12:766–772

Monshausen GB, Gilroy S (2009b) Feeling green: mechanosensing in plants. Trends Cell Biol 19:228–235

Monshausen GB, Bibikova TN, Weisenseel MH, Gilroy S (2009) Ca^{2+} regulates reactive oxygen species production and pH during mechanosensing in *Arabidopsis* roots. Plant Cell 21:2341–2356

Okada K, Shimura Y (1990) Reversible root-tip rotation in *Arabidopsis* seedlings induced by obstacle-touching stimulus. Science 250:274–276

Oliva M, Dunand C (2007) Waving and skewing: how gravity and the surface of growth media affect root development in *Arabidopsis*. New Phytol 176:37–43

Olson K, McIntosh J, Olmsted J (1995) Analysis of MAP 4 function in living cells using green fluorescent protein (GFP) chimeras. J Cell Biol 130:639–650

Paredez AR, Somerville CR, Ehrhardt DW (2006) Visualization of cellulose synthase demonstrates functional association with microtubules. Science 312:1491–1495

Richter GL, Monshausen GB, Krol A, Gilroy S (2009) Mechanical stimuli modulate lateral root organogenesis. Plant Physiol 151: 1855–1866

Rutherford R, Masson PH (1996) *Arabidopsis thaliana* sku mutant seedlings show exaggerated surface-dependent alteration in root growth vector. Plant Physiol 111:987–998

Schwab B, Mathur J, Saedler RR, Schwarz H, Frey B, Scheidegger C, Hulskamp M (2003) Regulation of cell expansion by the distorted genes in *Arabidopsis thaliana*: actin controls the spatial organization of microtubules. Mol Genet Genomics 269:350–360

Sedbrook JC, Kaloriti D (2008) Microtubules, MAPs and plant directional cell expansion. Trends Plant Sci 13:303–310

Sugimoto K, Williamson RE, Wasteneys GO (2000) New techniques enable comparative analysis of microtubule orientation, wall texture, and growth rate in intact roots of *Arabidopsis*. Plant Physiol 124:1493–1506

Telewski FW (2006) A unified hypothesis of mechanoperception in plants. Am J Bot 93:1466–1476

Thitamadee S, Tuchihara K, Hashimoto T (2002) Microtubule basis for left-handed helical growth in *Arabidopsis*. Nature 417: 193–196

Tsai YC, Delk NA, Chowdhury NI, Braam J (2007) *Arabidopsis* potential calcium sensors regulate nitric oxide levels and the transition to flowering. Plant Signal Behav 2:446–454

Yuen CYL, Pearlman RS, Silo-Suh L, Hilson P, Carroll KL, Masson PH (2003) WVD2 and WDL1 modulate helical organ growth and anisotropic cell expansion in *Arabidopsis*. Plant Physiol 131: 493–506

Yuen CYL, Sedbrook JC, Perrin RM, Carroll KL, Masson PH (2005) Loss-of-function mutations of root hair defective suppress root waving, skewing, and epidermal CFR in *Arabidopsis*. Plant Physiol 138:701–714